Analyzing Optical Properties of TiO_2 Amorphous and Polymorphs Forms

Cameron Stewart

An undergraduate thesis advised by Dr.Janet Tate

submitted to the Department of Physics,Oregon State University

in partial fulfillment of the requirements of the degree BSc in Physics

Submitted on May 15,2020

List of Figures

Contents

1 Abstract

The optical properties of Titanium dioxide(TiO_2) thin films vary based on if the oxide is in an amorphous or crystalline state as well as the thickness of each film. When crystalline, TiO_2 can be formed into three pol distinct polymorphs: rutile, anatase, and brookite. These crystalline phases are not present in the amorphous state so knowing phases of amorphous precursors is valuable information. With recent developments, known parameters can be used to create amorphous precursors that can have their crystalline phases known before annealing these thin films as well as thicknesses. To determine these optical properties, transmission and reflection spectroscopy was performed over the wavelength range 200 nm to 1000 nm.

Previous research had shown that absorption observed in the longer wavelength range (¿ 600nm) was strong for brookite and rutile thin films. This was observed for TiO_2 thin films of different thicknesses and different phase combinations. This paper expands upon these findings by exploring pure phase TiO_2 thin films that possess similar thicknesses. This would try to account for the correct error when determining absorption coefficients. Performing a Tauc Analysis would provide the bandgap energies for these films.

The same observance of absorbance in the long wavelengths was found in the pure phase films. Anatase absorbed very little with rutile absorbing the most and brookite slightly less. This follows the reasoning that defect states found in the amorphous films are present with films of similar thickness and in pure phase. The Tauc Analysis indicates that there is a decrease in energy for anatase and brookite when modeling them as a direct bandgap. This discovery did not carry over to the indirect bandgap analysis where on average the values remained the same.

2 Introduction

2.1 Goal

Titanium Dioxide(TiO_2) has been a widely studied in the material science community[1]. The applications vary from having self cleaning properties to being hydrophilic when lit up by UV light and hydrophobic in a light deprived environment[2]. To make the oxide viable for commercial use, the band gap, index of refraction and the allotropic forms must be fleshed out in understanding of how they work. Depositing TiO_2 onto a substrate allows for easy analysis through either electrical or optical methods. Creating samples of similar thicknesses and atomic orientation is very difficult. Janet Tate's research group, the Tate Lab have been working to determine a effective method for producing these TiO_2 where we can predict the amorphous precursor's for thin film samples before annealing them. The method used by Okan Agirseven in the Tate lab for producing these thin films is RF sputtering currently[3]. Recently he has managed to determine parameters to set where the amorphous precursors are known ahead of time. This has allowed him to produce films of similar thicknesses made up of 100% of each allotroptic form of TiO_2. Patrick Berry performed transmission(T) and reflection(R) measurements for films with some pure phase however these films were of different thicknesses[4]. The goal of this project was to determine how the optical properties vary across the allotroptic forms when now being able to produce them at the same thickness.

2.2 Optical Properties of Thin Films

RF Sputtering allow molecules to be deposited onto a substrate surface uniformly[6].This uniform deposition ensuring testing at any position along the materials surface provides similar results. TiO_2 is a oxide semiconductor that can be deposited with this technique, onto Silica (SiO_2) substrates. When deposited onto Silica, the TiO_2's molecular structure has long-range disorders. This is known as the amorphous form of TiO2 Rearranging this state requires annealing the molecular structure reforming the TiO_2 into a crystalline state in any variation of three polymorphs. These polymorphs include brokite, rutile, and anatase as seen in figure 2.1 . Each one is made up of the molecule TiO_2 however their geometric arrangement of Ti and O_2 will vary. Due to this chemical variance, the three polymorphs, bandgap, transmission of light, reflection of light, and index of refraction will also differ.

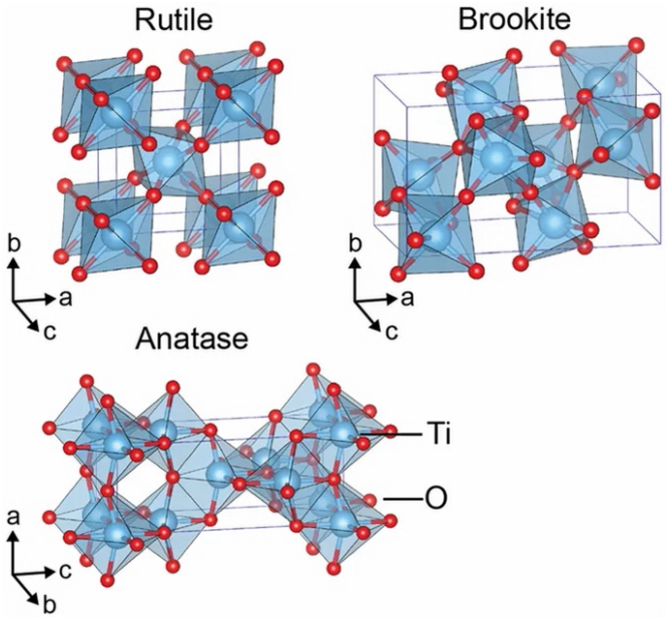

Figure 2.1: Polymorphous forms of Titanium Dioxide with the red dot representing the oxygen atoms and the red the titanium atoms.[5]

RF Sputtering is a effect method for creating TiO_2 made up of a smooth layer with a combination of any of the three polymorphs. The issue that has arisen is the amorphous precoursers of TiO_2 can be made up of any random combination of brookite, rutile and anatase using modern methods. The inability to make a sample with predetermined specifications prevents efficient analysis of TiO_2. With however recent developments as of Okan Agirseven, these amorphous precursors can be determined before the process of anneal which reforms the disorder molecular chains to clearly organized long order chains. Since each polymorph possesses different optical properties, creating parameters so for example a sample is made of 100% of anatase would provide easy examination of how the bandgap changes for a sample of 100% of brookite.

2.2.1 Refractive Index and Transmission and Reflection

All electromagnetic radiation propagates through a vacuum at the speed of light. As light approaches a medium other than a vacuum, the speed decreases. This change in speed is classified by the Refractive Index, a ratio which takes the quotient of the speed of light in a vacuum divided by the speed in a different medium.

$$c = \frac{n}{v}, \tag{1}$$

c is speed of light = $3 \times 10^8 \ \frac{m}{s}$ and v is the speed of light through a medium. The value for n in is the real component of the refractive index which is accompanied by an imaginary component κ . Therefore, the complex refractive index is,

$$n = n_{real} + i\kappa, \tag{2}$$

The imaginary component κ is the extinction coefficient which accounts for the attenuation as the light travels through a new medium. An attenuation in optics is the gradual loss of intensity which the light experiences. This attenuation includes the scattering of light and the absorption from the medium the light travels through. TiO_2 for example contains an absorption between the wavelengths of 300nm to 400nm. This absorption is known as the bandgap which will be further discussed in a later section. The drop of the flux density occurs as a rate of e^{-1}, where the wave travels the distance y

$$y = \frac{1}{\alpha}, \tag{3}$$

which is the penetration depth within the material[7]. For TiO_2, this distance is big enough that the material can be transparent as its thickness is much less in terms of length. To calculate the real part of the index of refraction, an equation known as the Sellmeier equation can used to determine its value

$$n^2(\lambda) = 1 + \sum_i \frac{B_i \lambda^2}{\lambda^2 - C_i}, \tag{4}$$

where B_i and C_i are values that must be experimentally determined with varying λ(wavelength) values. The imaginary component can be found from

$$\kappa = \frac{\alpha \lambda}{4\pi}, \tag{5}$$

where alpha is the absorption coefficient. Looking at the behavior of light interacting with a medium other than a vacuum, there is absorption as well as the transmission of light and reflection. The transmission of light is the amount of radiation that propagates through the medium and exits outside of the opposing side. TiO_2 visually is clear to be transparent which allows a large portion of the light to transmit through.

The rest of the light must get reflection after the incident light interacts with the medium. Combining the absorption, transmission, and reflection should equal the flux before the light interacted with the medium. T and R spectroscopy is a direct way that the transmission and reflection can be measured.

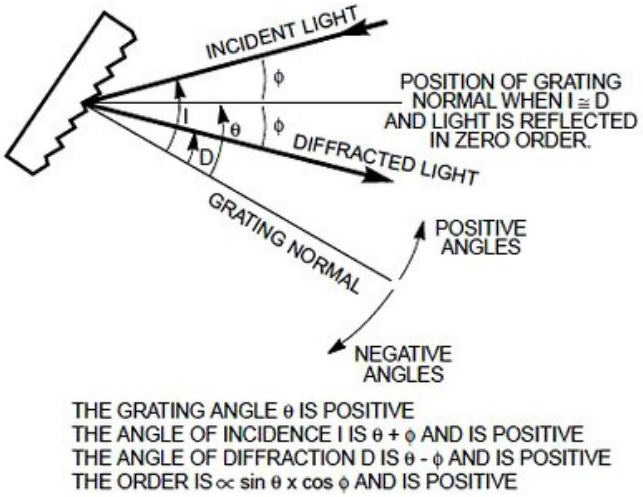

Figure 2.2: Diffraction Grating of an Incident Monochromatic Light source[8]

Using diffraction grating, in figure 2.2, the incident light approaches the grating then once the two interact, the light gets emitted back out into the medium. The angle the light hits the grating will determine the wavelength of light that gets emitted. For this project, by using this technique the wavelength of light can be generated across a range of wavelengths.The incident light is made up of the T and R

$$I = T + R + A, \tag{6}$$

where A is the absorption. This reflection and transmission data can then be plugged into a formula confirmed by

$$\frac{T}{(1-R)} = e^{-\alpha d}, \tag{7}$$

determining the α (absorption coefficient) and d (width of material) becomes doable once these transmission and reflection values are found[9].

2.2.2 The Bandgap

TiO_2 has a bandgap of 3.2 to 4.0 eV which is determined experimentally using spectroscopy. The bandgap must be small enough that the electrons can transition from the valence band to the conduction

band[11]. The valence band is the region where the electrons would be and when the energy needed to leap to the conduction band is met, the empty “holes” in the conduction band are filled.

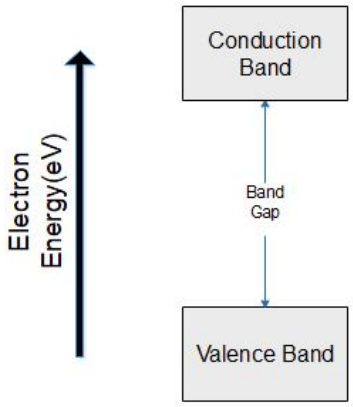

Figure 2.3: Bandgap in between the valence band and conduction band. The bandgap rising in terms of electron energy expressed in electron volts

The electrons need energy to make the jump between the two bands as seen in figure 2.3. One method is exciting the electrons by sending light to the semiconductor. This energy measured in electron volts(eV) increases as you jump from the valence to the conduction band. Similarly in order to drop from the conduction to the valence band there would need to be a release in energy. In certain cases this energy comes off as photons of light.

2.3 Interference Fringes: Destructive and Constructive Waves

As light interacts with a new medium, the wave will either reflect off the medium’s boundary or transmit through. The amount of light flux transmitted over the incident flux determines the transmittance. The reflectance is the same except the ratio of the reflected lights flux and incident light is taken. In figure 4, the electric field(E_{0i}) travels in the same direction as the incident waveform. After interacting with the first layer of TiO_2, the reflected light will experience a π phase shift due to interacting with a medium of higher index of refraction.

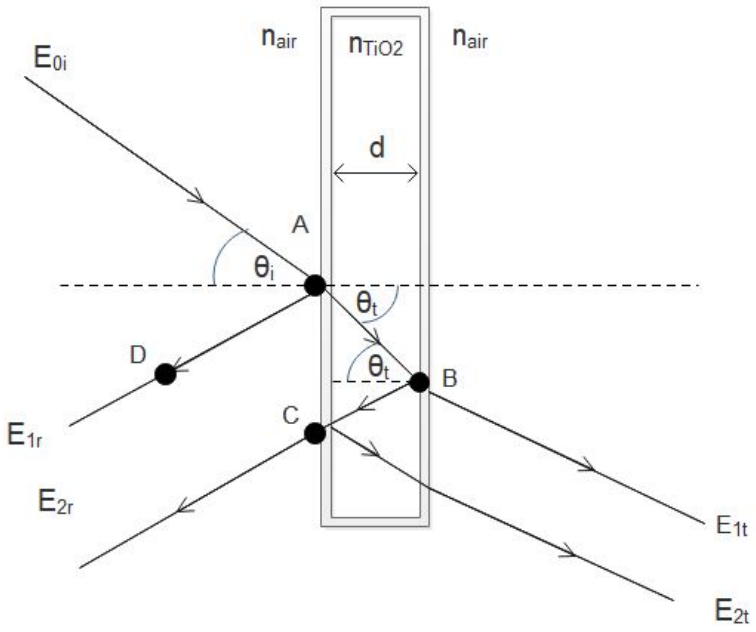

Figure 2.4: Change==Light interacts with the TiO_2 sample first transmitting and reflecting off of the TiO_2 sample. The transmission light interacts with the SiO_2 substrate transmitting once again with the light reentering air and reflecting the other portion of light through the TiO_2 then out to air

Due to the phase shift the reflected light,there will be optical length difference(OPD. In equation 7, the OPD is represented using the thin film seen in figure 2.4 for the first reflected light wave.

$$\Lambda = n_{TiO_2}(AB + BC) - (AD)n_{air} \tag{8}$$

Expanding this to an m number of interference's will result in equations 9 and 10. One where the two waves interfere constructively seen in equation 9 and one where they destructive interfere seen in equation 10 c

$$2nTiO_2dcos(\theta_t) = (m + \frac{1}{2})\lambda_0 \tag{9}$$

$$2nTiO_2dcos(\theta_t) = (m)\lambda_0 \tag{10}$$

In experimental work these interference patterns will appear as fringes in the reflectance data. The fringes with a maximum of reflectance will infer a minimum in the transmittance and visa versa. This detail will important for analyzing the transmission and reflection data.

3 Materials and Methods

3.1 Grating Spectrometer

The in house grating spectrometer Dr.McIntyre's lab measures the transmission and reflection of incident light after passing through thin films. The spectrometer requires a xenon lamp light source powered by a LPS 251 Lamp Power Supply. An ozone eater is attached to the rear of the lamp to prevent ozone from leaking into the nearby environment caused by the ultraviolet radiation projected by the lamp. The light from the xenon lamp, contains wavelengths from 185nm to 2000nm[10]. Realigning

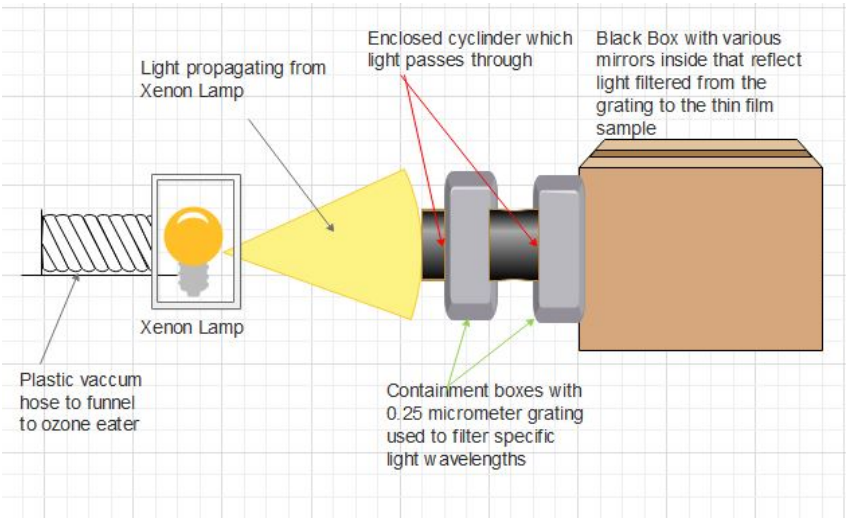

Figure 3.1: Broad view of spectrometer experimental layout

the grating angle to the incident light changes which wavelengths reflect from the gratings surface. The first containment seen in figure 3.1, will filter out wavelengths except for ones between 200nm to 1000nm while the second filters out the light again by 1nm increments within the previously mentioned range. Light enters the black box through a 13.6mm opening and then gets magnified by a convex lens. A mirror redirects the light by 90 degrees in the counterclockwise direction.An iris is position afterwards to alter the amount of area the light passes through a circular opening. Thin films are placed in a stand and aligned with the light passing through the iris.

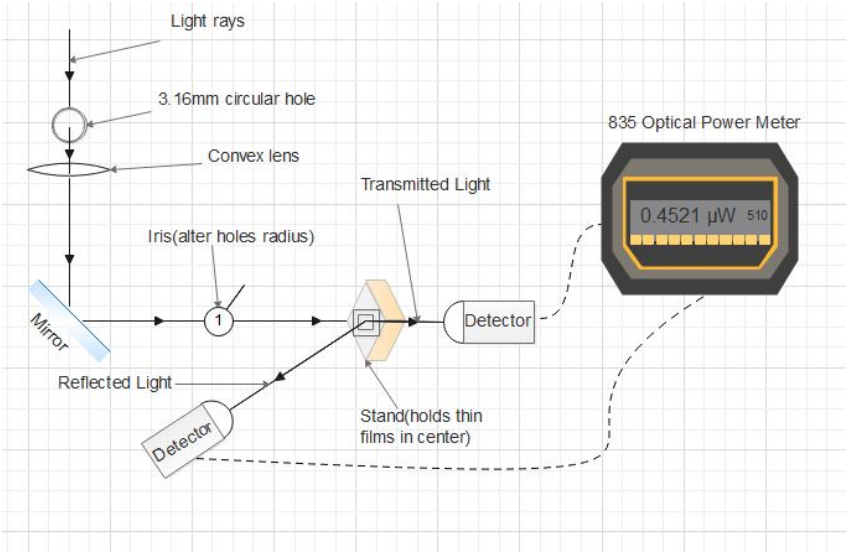

Figure 3.2: Optical layout inside the black box including the 835 Optical Power Meter

The transmission and reflection of light were recorded in units of voltage with the Si-detector.To properly quantify the data, the total voltage of light before any

To utilize this light for measurements, a optical power detector with a circular lens allows light to transmit through which then travels through a fiber optic cable to a 835 Optical Power Meter. This setup is seen in figure 3.2 where the power output was measured in terms of watts. This detector has two positions, one for the transmission and one for the reflection of the thin films.To analyze this data, the proprietary software known as LabVIEW is used to store the transmission and reflection data.Graphs are plotted with this data in LabVIEW and also exported into an Excel notebook known as Index Calc

3.2 Error due to alignment

The majority of the spectrometer's orientation remains fixed, however with each new film the light reflected will produce a different reflection angle. The transmission is unaffected continuing along the same path as the incident light. To account for this angle difference in each film, the stand holding the TiO_2 can be rotated horizontally and vertically. Aligning the reflected light with the detector properly is imperative for consistent and accurate results.

3.3 Index Calc

The transmission and reflection data collected from LabVIEW can be imported into a excel notebook made by James Haggerty known as Index Calc. The main purpose of this notebook is to use the transmission and reflection data to determine the thickness and index of refraction for TiO_2. The reflection graph displayed in Index Calc places the experimental data along with a fitting curve. This fitting curve is dictated by the fringes at different wavelengths as well as the thickness of the thin film. The fringe values are recorded into the notebook and a guess for the thickness are the preliminary values needed to approximate the fit. Two buttons control the first step of the fitting, first by using the fringes to find a reasonable thickness and second doing the reverse. Iterating over these two buttons over time produces a better fit to the experimental data.

3.4 Tauc Analysis

To determine the bandgap values, a process known as a tauc analysis was performed. Figure 3.3 presents an example of the plots produced from the analysis. The curves change as a function of energy in electron volts. The y axis is this energy multiplied by the absorption coefficient. For the direct bandgap, the (αE) value is raised to a half and for the indirect it was raised to $\frac{1}{2}$. The linear behavior seen in certain ranges of energy, is where a linear fit is placed and extrapolated to the x axis. This done to determine the onset absorption which will occur just before the linear increase.

The urbach tail, which is the exponential portion of the curve to the left side of the linear absorption curve. This portion can occur due to localized states that mix into the bandgap. This establishes the reasoning for making the linear fit extrapolate before the exponential drop off which would provide a inaccurate bandgap value.

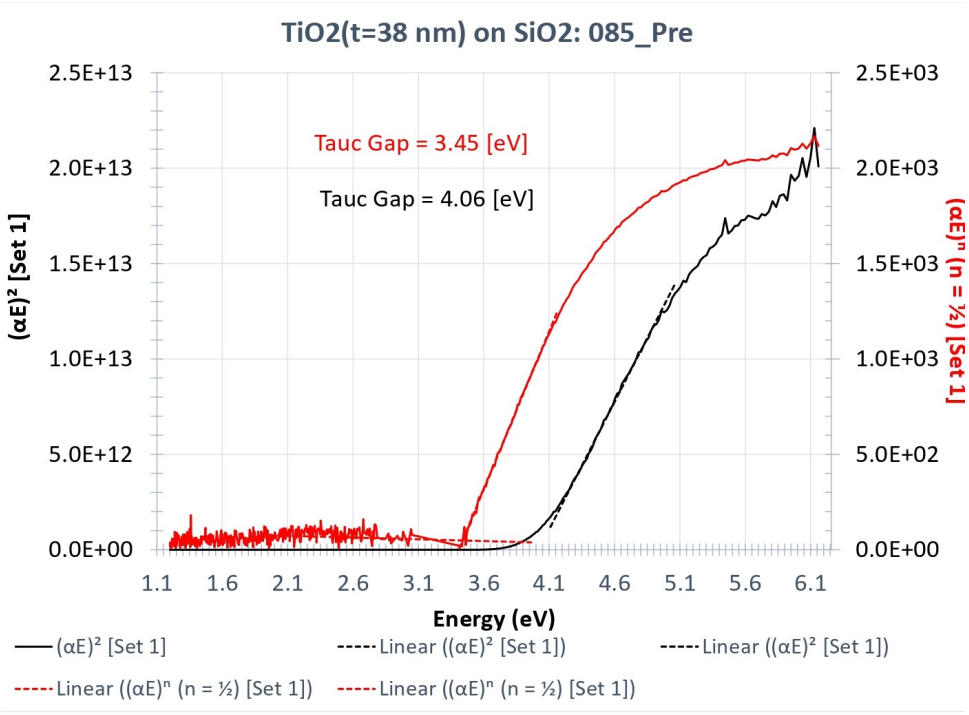

Figure 3.3

3.5 O_2 deficiency

Sample #	O_2(at %)	pO_2
TiO2_S_065_Pre(rutile)	0.63	1.67
TiO2_S_065_Post(rutile)	0.65	1.67
TiO2_S_072_Pre(brookite)	0.64	2.86
TiO2_S_072_Post(brookite)	0.65	2.86
TiO2_S_085_Pre(anatase)	0.66	2.86
TiO2_S_085_Post(anatase)	0.65	2.86

Table 1: Thickness and bandgap for thin film rutile, anatase, and brookite samples

Using a electron probe micro-analyzer (EPMA), Okan Agirseven from the Tate lab was able to determine the oxygen percentage portion for the thin films. Table 1 shows us that the O_2 was highest in the anatase pure phase sample. With a higher oxygen content, there are less electron holes to be filled up and absorbed.

4 Results and Discussion

Transmission and reflection measurements were recorded for 24 samples of TiO_2 on a SiO_2 substrate, which includes the amorphous and crystalline forms. Using T and R, the film thickness, index of refraction at 633nm and the bandgap were all determined. The following plots and data will be labeled in colors, blue for brookite, red for rutile and green for anatase polymorphs.

Sample #	Minimization Parameters ($X^2[R], X^2[T]$)	Film Thickness(nm)	n @ 633nm	Sellmeier error
050 _Pre	0.22,0.31	43.9	2.43	0.25
051_Pre	0.9, 0.37	34.2	2.43	0.73
051_Post	0.01, 0.14	34.9	2.53	0.94
052_Pre	0.87, 0.92	25	2.45	0.25
052_Post	0.99, 0.64	23.1	2.68	0.90
053_Pre	0.48, 0.40	26	2.08	0.30
053_Post	0.62, 0.52	28.95	2.22	0.09
054_Pre	0.83, 0.96	26	2.19	0.56
054_Post	1.95, 2.21	29.9	2.01	0.67
060_Pre	0.81, 0.46	20	2.64	0.67
060_Post	1.4, 0.78	21	2.6	0.47
065_Pre	0.95, 0.15	45.0	2.36	0.18
065_Post	1.2, 0.73	40.2	2.35	0.75
068_Pre	0.97, 0.50	55.1	2.46	0.34
068_Post	0.8, 0.46	25.0	2.38	0.39
072_Pre	0.4, 0.75	27.0	2.6	0.51
074_Pre	0.53, 0.30	54.9	2.37	0.63
074_Post	0.98, 0.44	55.1	2.45	0.98
077_Pre	0.84, 034	128.1	2.47	0.34
077_Post	0.88, 0.37	127.0	2.53	0.22
085_Pre	0.25, 0.24	38.0	2.53	0.75
085_Post	0.86, 0.29	38.0	2.54	0.89
086_Pre	0.69, 0.16	165.1	2.46	0.07
086_Post	0.85 , 0.28	164.7	2.51	0.34

Table 2: Thickness and bandgap for thin film rutile, anatase, and brookite samples

Table 2 is the list of TiO_2 pre and post anneal samples, each had transmission and reflection mea-

surements recorded over the wavelength range 200-1000 nm. The minimization parameters provide a value to indict the amount of error when fitting to the transmission and reflection data. Values less than 1 provide the best fit, between 1 and 2 is considered a good fit, and values over 2 indicate a bad fit. The thicknesses varied on accuracy based on these minimization parameters. The refractive indices were found from altering the sellmeier coefficants that makes up the sellmeier equation. A similar minimization parameter was recorded for the sellmeier coefficients fitting the index of refraction curve depicted by the fringe data input into Idex Calc. The thickness and refractive indices were compared with ellipsometry data found by the Tate Lab from Joseph Kreb, which can be found in the appendix.

4.1 Transmission and Reflection

The calculated transmission and reflection measurements produced graphs as seen in figure 4.1 with sample TiO_2_086_Pre. The expected corrected transmission should follow equation 6 where the light exists in transmission, reflection or absorbance. This follows the law of energy conservation, where all the energy before interacting with the system must be retained in the thin film through one of these three behaviors. For Sample 86_Pre, between 200-320nm, around 30% of intensity from the reflection, 0% from transmission, indicating the remaining portion of light is absorbed. This area of high absorption is where the bandgap exists. After this region, the reflection of light and transmission are much higher with the absorption values dropping significantly as the wavelength increases to 1000nm. From Eqn 6, $\frac{T}{1-R}$ hovers at 90% of the raw intensity of light. Therefore we can conclude that a portion of the intensity is absorbed however it is not due to the bandgap. One possible reason is the defect states present could produce an absorption outside the bandgap.

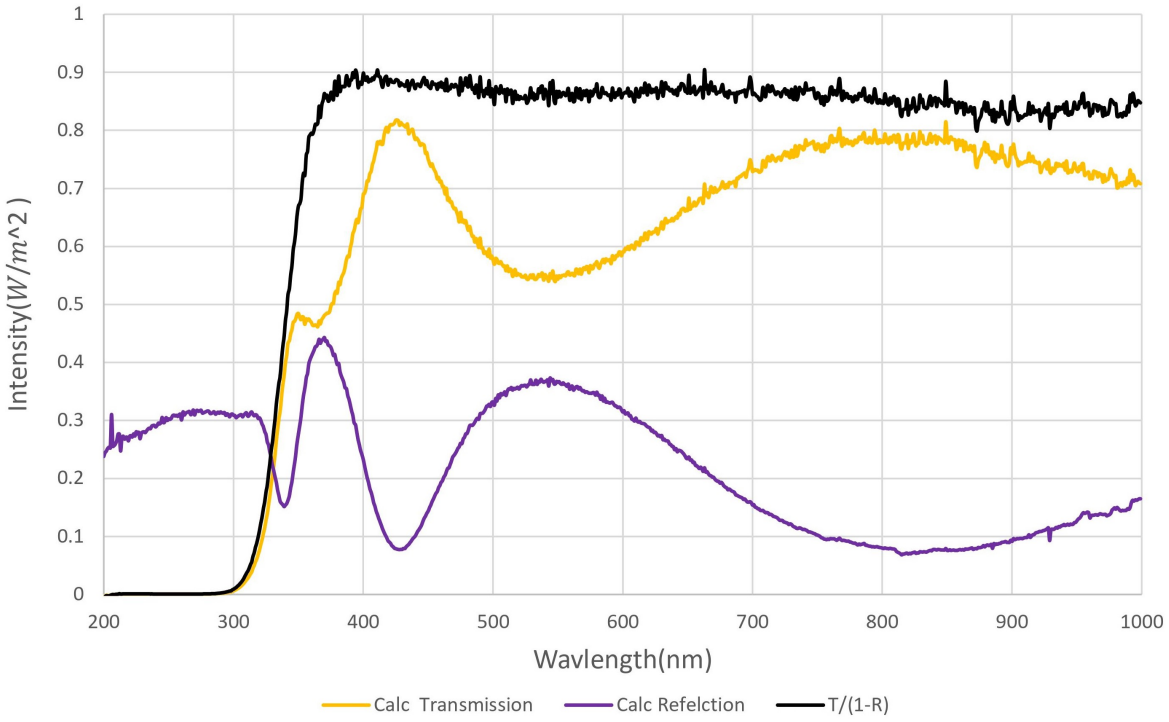

Figure 4.1: $\frac{T}{1-R}$ graph for all samples measured

The SiO_2 substrates were used due the samples low absorbance across the UV-VIS-NIR spectrum. Looking at figure 4.2, the transmission hovers at 92% from 220nm to 1000nm and the reflection contains the other 8% of light. Some noise appears between 200-220nm in the SiO_2 intensity plot. The intensity exceeding 100% indicates a misalignment of the incident beam. If there was some absorption within this region, that would carry over to the TiO_2's intensity plot seen in figure 7. So we can conclude that the SiO_2 substrate has a negligible effect on the absorption seen within the UV-VIS-NIR spectrum.

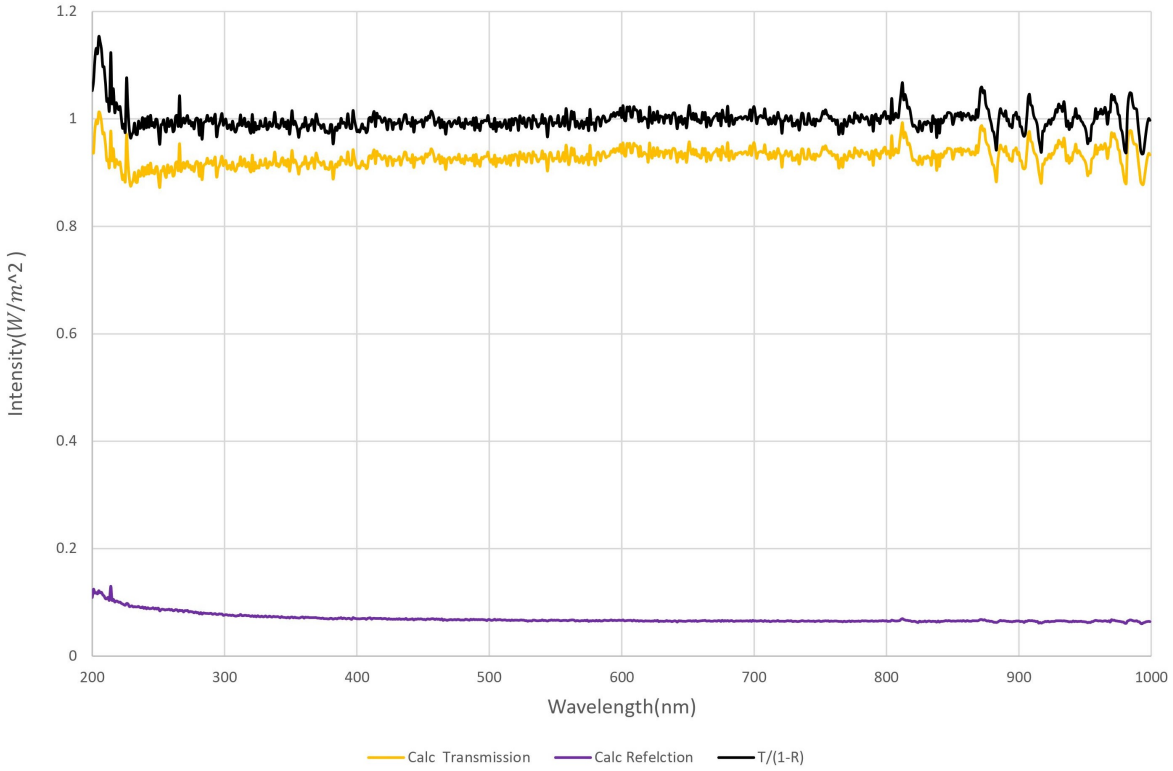

Figure 4.2: $\frac{T}{1-R}$ graph for all samples measured

Now that both the transmission and reflection behavior for the substrates and thin films are established, we want to try and find some distinction between the films. The thickness, atomic arrangement, and amorphous precursors are three physical properties that directly affect the optical properties. A method for analyzing these affects is plotting the pre and post anneal $\frac{T}{(1-R)}$. These plots can be seen in figure 4.3 and 4.4, where the rutile, brookite, and anatase are indicted as mentioned previously by their distinct color choice. With the pre anneal samples in figure 4.4, we view a variety of samples measured with clear curves with only visible noise in the rutile curve around 800-1000nm's. There is a clear trend of rutile samples transmitting less than brookite and anatase in the 350-1000nm wavelength range. Brookite transmits better than the rutile sample and anatase overall has the best transmission in this range.

After annealing the structure of the TiO_2 becomes highly ordered. In the post anneal seen in figure 4.4, we see the brookite samples increase in transmission in between 350-1000nm, going from around 95% up by about 3 to 5%. The only sample which still observes a high absorption in this range is the rutile sample. In table 1 we observed the O_2 content increase for brookite and rutile films when transitioning from amorphous to crystalline. The anatase films decrease in oxygen content, which at

this moment we don't have an explanation for.

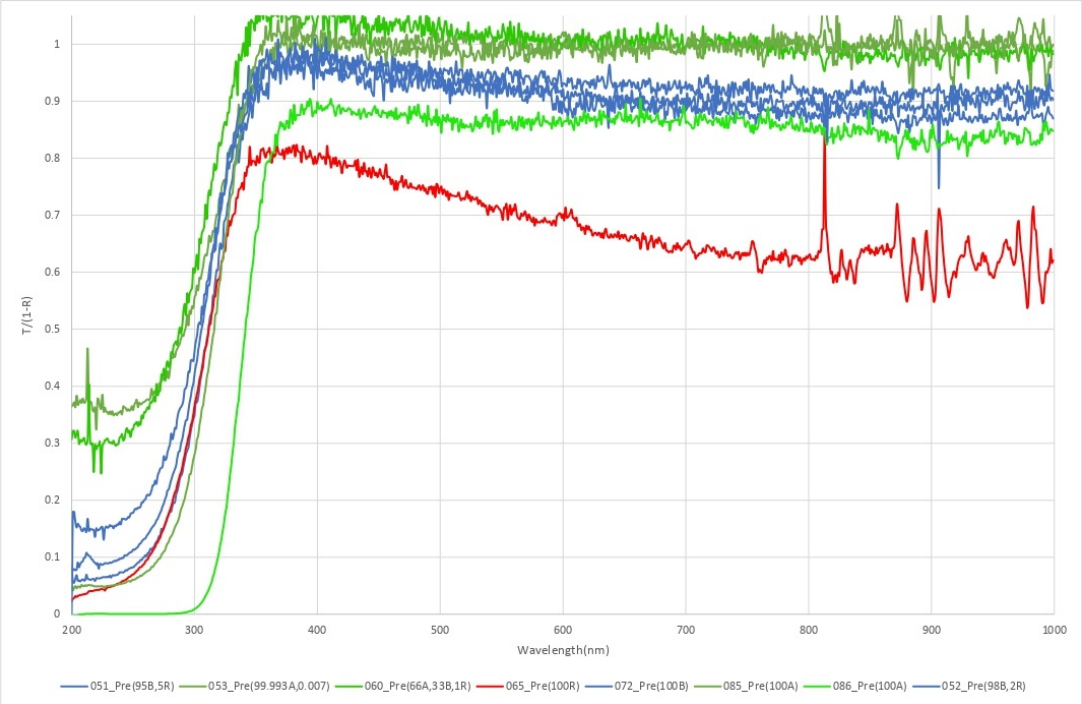

Figure 4.3

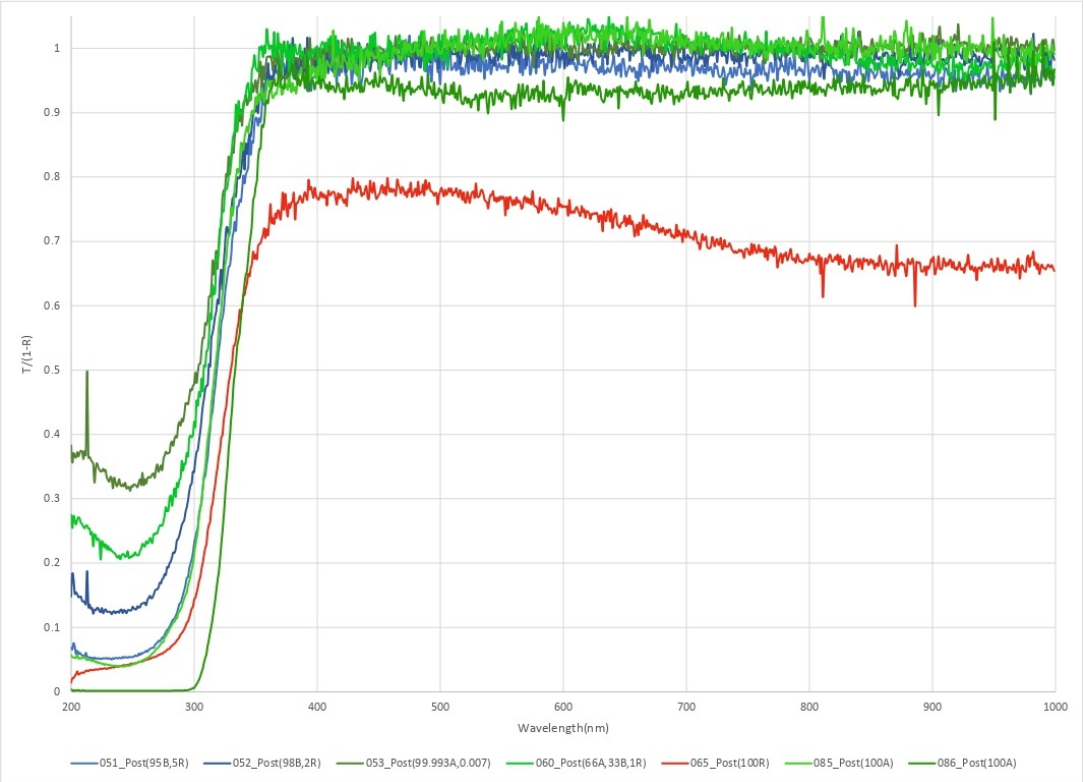

Figure 4.4

The correlation however between brookite and rutile growing in transmission as well as O_2 content

seems to hold as a possible reason for the absorption observed in the 350-1000nm range. The crystalline films become more oxygen full therefore this causes a decrease in absorbance and a increase in transmission.

4.2 Absorption Coefficient

In figure 4.5 and 4.6, we see the respective absorption coefficient values as a function of the wavelength calculated with equation 7. We can more clearly distinguish the absorbance of each sample. Anatase has values of absorbance coefficients ranging from 0 to 10,000 cm^{-1}. There is one sample, 60_Pre which most likely was not properly aligned during the experiment causing unrealistic behavior of a negative coefficient number. The pre anneal brookite samples resided much higher betwen 10,000 to 40,000 cm^{-1}. Rutile values were the highest go from 40,000 cm^{-1} up to 110,000 cm^{-1}. These samples were determined to be at a variety of thickness measurements however there are clear sections defined for each polymorph. This indicates that the coefficents regardless of thickness are restricted to specific values, only scaling up or down within this region by their thickness.

Figure 4.5

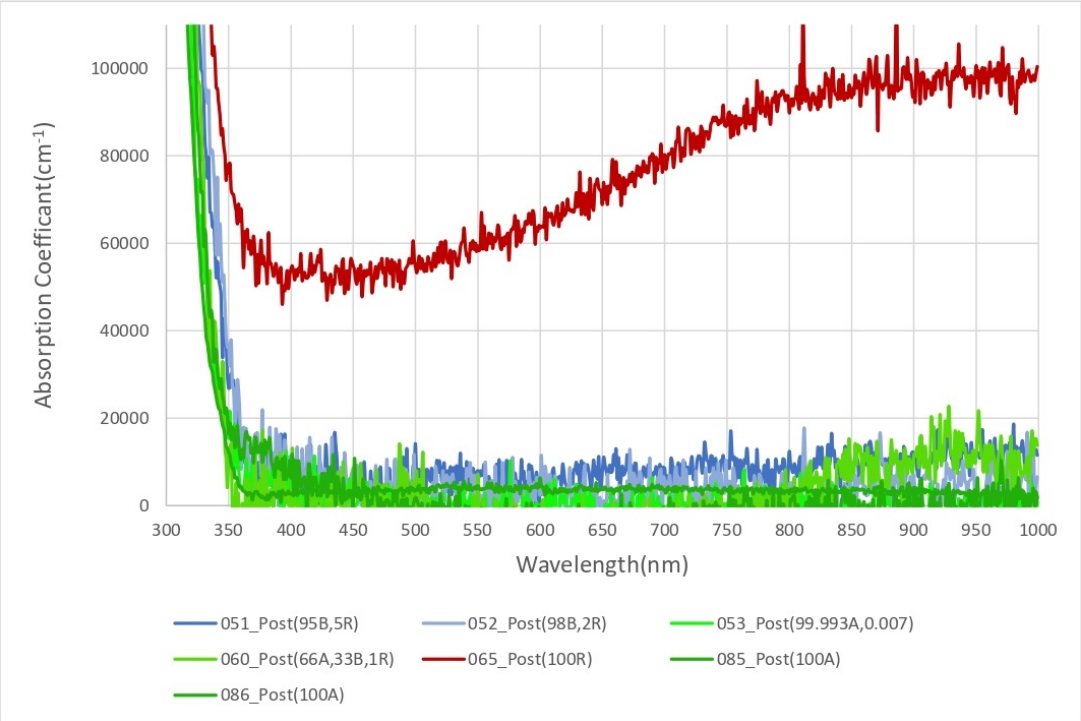

Figure 4.6

4.3 Pure Phase Films

All the $\frac{T}{(1-R)}$ curves shown so far are from samples with various thicknesses and phase fraction percentages. Samples 65, 72, and 85 were all produced with 100% phase refractions of each polymorph. These curves in figure 4.7, were plotted with both pre and post anneal samples of TiO_2. For sample 65, which was 100% rutile, the thickness measurements were 45nm for the pre and 40.2 for the post. The anatase sample was 85, which for pre and post were both essentially 38nm. Due to the current situation with the pandemic, sample 72 pre was only measured with no comparison to the post for this analysis. With the brookite and anatase samples isolated around the same value thickness, the effects of the thickness should be negligible to the curves. In this figure,it is more clear that rutile tends to absorb around the 60-70% range for wavelengths 800-1000nm. The anatase samples were clearly the least absorbent as expected with transmissions around 100% recorded for wavelengths 400-1000nm. These plot show that when considering thickness independence, the phase each polymorph is made of will affect the absorbance seen between 400-1000nm.

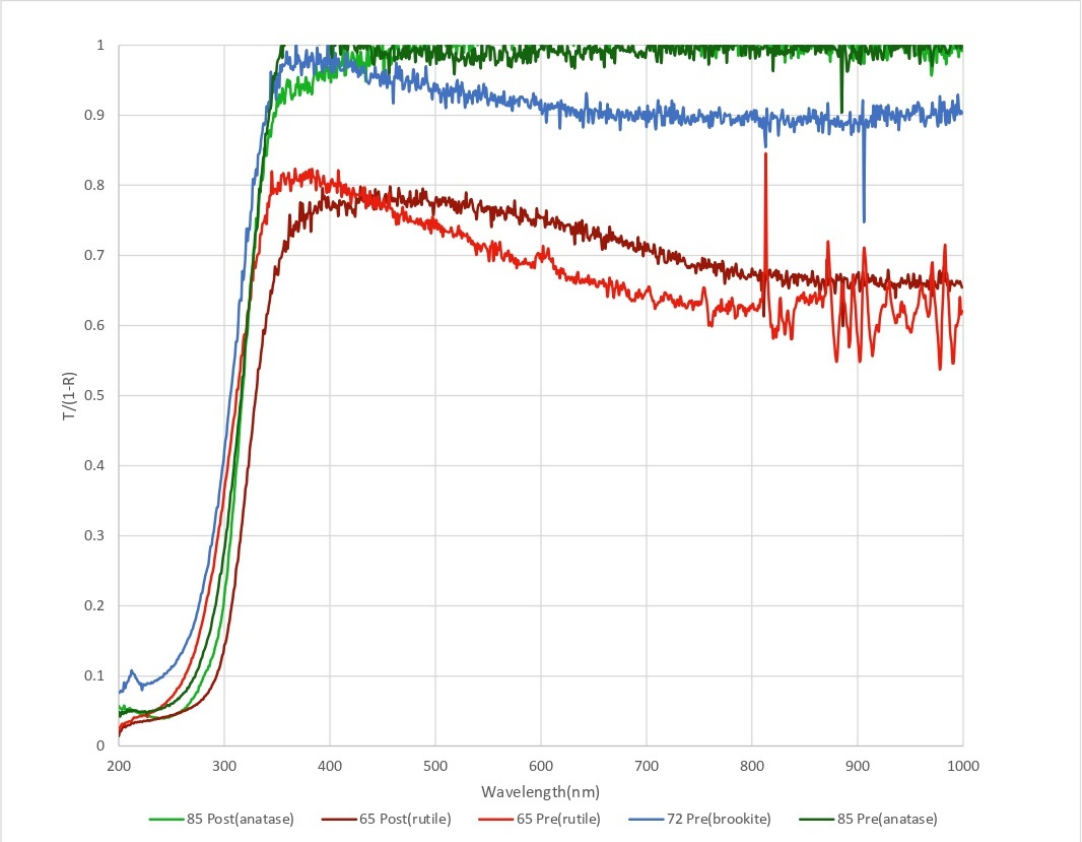

Figure 4.7: $\frac{T}{1-R}$ plots for samples 85 pre and post, 72 pre, and 65 pre and post. The expected trend is that anatase transmits or reflects nearly 100% of light at wavelengths beyond the bandgap range(250-350) followed by a slightly absorbent brookite than finally rutile absorbing the most past this. This also helps further display the effects of O_2 deficiency on the absorbance seen outside of the bandgap.

4.4 Band Gap Analysis

A Tauc analysis was performed for each sample to find the indirect and direct bandgap values. The goal was to formulate any unique behavior that occurred with the samples. In table 3, the calculated values for each sample were found for all 24 samples. Initially the behavior seen was a decrease in the bandgap energy was observed for the indirect and direct. Certain samples however experienced a significant increase in energy after the annealing process. Only one direct bandgap sample, 86 increased from 3.9 eV to 4 eV. The indirect bandgap values were a mixture of increasing, decreasing, and remaining the same. There was not clear distinction, unlike the direct bandgap with a clear decrease on nearly all the thin films.

Sample 86 was the thickest film at 165.1 nm pre anneal, sample 77 however was also relatively thick compared to the other films at 128.1 nm in the amorphous state and did not experience the same increase. The other corresponding 100% anatase phase samples to 86, all decreased in energy after

the annealing process. There was not any discernible property for samples which increased in energy and those that decreased. None of the unique properties appeared to play a role including the thickness and crystalline phase composition.

Sample ID #	Direct Bandgap(eV)	Indirect Bandgap(eV)
050_Pre(95A,5B)	4.1	3.4
051_Pre(95B,5R)	4.1	3.5
051_Post(95B,5R)	4	3.6
052_Pre(98B,2R)	4.1	3.5
052_Post(98B,2R)	4.0	3.4
053_Pre(99.993A,0.007)	3.9	3.3
053_Post(99.993A,0.007)	3.8	3.4
054_Pre(96B,4A)	4.1	3.6
054_Post(96B,4A)	3.8	3.5
060_Pre(66A,33B,1R)	4.0	3.5
060_Post(66A,33B,1R)	3.9	3.5
065_Pre(100R)	4.2	3.6
065_Post(100R)	3.9	3.6
068_Pre(100A)	4.0	3.4
068_Post(100A)	3.9	3.5
072_Pre(100B)	4.1	3.6
074_Pre(90.5B,9.5R)	4.2	3.4
074_Post(90.5B,9.5R)	4.0	3.4
077_Pre(63B,37R)	4.1	3.5
077_Post(63B,37R)	4.0	3.5
085_Pre(100A)	4.1	3.5
085_Post(100A)	4.0	3.4
086_Pre(100A)	3.9	3.4
086_Post(100A)	4.0	3.4

Table 3: Direct and indirect bandgap results in terms of electron volts(eV). While a polymorph can only possess either a direct or indirect bandgap, both were calculated as the mathematical process does not dictate which bandgap the thin film has.

Phase Anneal State	Direct Bandgap(eV)	Indirect Bandgap(eV)
Anatase-Pre	4.0	3.4
Anatase-Post	3.9	3.4
Brookite-Pre	4.1	3.5
Brookite-Post	4.0	3.5

Table 4

In table 4, there are the average bandgap values determined for the anatase and brookite thin films. Rutile was not considered as there was only one sample, so a average would be nonsensical. The pre annealed state films on average produced higher direct bandgap values than the post annealed films. This behavior did not carry over to the indirect where the average was the same for pre to post for both sets of samples. There is not any indication on why the small shift was present in the direct bandgap analysis and not the indirect. The change could be related to the defect states which were shown to be a possibly affecting the long wavelength regions however this is simply speculation.The presented data does not provide enough evidence to determine the cause for the possible decrease in energy found with the direct bandgap results.

5 Conclusion

TiO_2 has proven to be useful for its self cleaning properties, ability to repel water when under the influence of ultraviolet light, and other uses. The process for developing TiO_2 onto SiO_2 did not have a defined model for creating samples with known amorphous precursors. With recent developments in the Tate lab, Okan Agirseven has developed a method for setting parameters to know the crystalline phase structures before the annealing process was performed on these films. By measuring the transmission(T) and reflection(R) using T and R spectroscopy, within the ultraviolet to near infrared range(UV-VIS-NIR), the thickness, absorption and refractive indices of the thin films were calculated. These T and measurements were recorded for the sputtered amorphous precursors and the corresponding crystalline films.

In the research preceding this project, Patrick Berry from the Tate Lab performed similar T and R measurements for TiO_2 thin films of various thicknesses and crystalline state phases. He was not able to measure samples of the three pure phase polymorphs that all around the same thickness. With this project, similar thickness films of pure phase were produced and measured for their T and R. The absorption in the longer wavelength range($>$ 600 nm) observed was also seen in previous results analyzed by Berry for mainly brookite and rutile samples.The current hypothesis is the oxygen deficiency create defect states that cause absorption in these long wavelengths. Results for $\frac{T}{1-R}$ indicate from pre to post anneal there is a decrease in absorption as more oxygen vacancies are filled.

Oxygen deficiencies is a reasonable explanation, more samples of pure phases at higher thicknesses would both provide a more concrete understanding of this behavior. The bandgap was explored for amorphous procurers and their crystalline form. Anatase films on average had a lower bandgap energy for the amorphous films for the direct and indirect bandgap compared to the brookite films. Rutile was not considered as the sample size was not enough to determine an average. The direct bandgaps experienced a average loss in energy from pre to post anneal. The indirect bandgaps experienced no loss in energy from pre to post anneal. There was not a clear indication on why this occurred and further research will likely provide a clearer explanation of this behavior observed. Overall, the goal to determine if similar thickness pure phase films produced results seen in previous research was a success and is open for further developments to be explored.

References

[1] Roy, P., Berger, S., and Schmuki, P. (2011). TiO2 Nanotubes: Synthesis and Applications. Angewandte Chemie, 50(13), 2904–2939. https://doi.org/10.1002/anie.2010013745

[2] Park, J. Y. (2018). How titanium dioxide cleans itself. Science (New York, N.Y.), 361(6404), 753–753. https://doi.org/10.1126/science.aau6016

[3] Agirseven, O., Rivella, D. T., Haggerty, J. E. S., Berry, P. O., Diffendaffer, K., Patterson, A., Kreb, J., Mangum, J. S., Gorman, B. P., Perkins, J. D., Chen, B. R., Schelhas, L. T., and Tate, J. (2020). Crystallization of TiO2 polymorphs from RF-sputtered, amorphous thin-film precursors. AIP Advances, 10(2), 025109. https://doi.org/10.1063/1.5140368

[4] Berry, Patrick (2019). Characterizing Optical Signatures of TiO_2 Precursors[Unpublished bachelor's thesis]. Oregon State University.

[5] Nair, Prabitha B., V. B. Justinvictor, Georgi P. Daniel, K. Joy, V. Ramakrishnan, and P. V. Thomas. "Effect of RF Power and Sputtering Pressure on the Structural and Optical Properties of TiO2 Thin Films Prepared by RF Magnetron Sputtering." Applied Surface Science 257.24 (2011): 10869-0875. Web.

[6] Haggerty, J. E. S., Schelhas, L. T., Kitchaev, D. A., Mangum, J. S., Garten, L. M., Sun, W., Stone, K. H., Perkins, J. D., Toney, M. F., Ceder, G., Ginley, D. S., Gorman, B. P., & Tate, J. (2017). High-fraction brookite films from amorphous precursors. Scientific Reports, 7(1), 15232. https://doi.org/10.1038/s41598-017-15364-y

[7] Hecht, Eugene. Optics. 3rd ed.,Addison-Wesley, 1998

[8] 2019. Diffraction Grating Physics. Retrieved from http://:www.newport.com/t/grating -physics

Measure R and T for sputtered amorphous precursor and corresponding crystalline films. Of different polymorphs of TiO2
New is that these films different polymorphs all have similar thickness, whereas in previous work (Patrick Berry) the films were orders of magnitude different in thickness. able to remove any effects due to thickness and to due difficulties in analuzing the thinner films. See same trend of increased absorption in the long wavelength region in rutile (esp) and in brookite rel to anatase.

DO all amorphous precursors have the same BG (by indirect gap)? or are different polymorphs different?
Doe BG (measured either by direct or indirect) changes from pre to post in each polymorph. If yes, does it correlate with anything?

NO -> appendix. Consistency with uv-nir spectroscopy and ellipsometry for d and n.

Figure 5.1: Plot of all the direct and indirect values found with a Tauc Analysis. These values were placed on a arbitrary x axis.

[9] Y. Hishikawa, N. Nakamura, S. Tsuda, S. Nakano, Y. Kishi, and Y. Kuwano, Jpn. J. Appl. Phys., Part 1 30, 1008 (1991). https://doi.org/10.1143/jjap.30.1008

[10] Iguchi,T., Patel,S., Lares, M.,& Hamamatsu Corp. (2010, October 8).A Guide to Selecting Lamps. Retrieved January 3, 2020, from https://www.photonics.com/Articles/A_Guide_to_Selecting_Lamps/a44487.

[11] Casiday,Rachel,et al."Bonds,Bands,and Doping:How Do LEDs Work?."Washington University in St. Louis,Department of Chemistry.¡ http://www. chemistry. wustl. edu/ courses/genchem/Tutorials/LED/bands06. htm (2007).

6 Appendix

6.1 Section 1: Ellipsometer vs Spectrometer Comparison

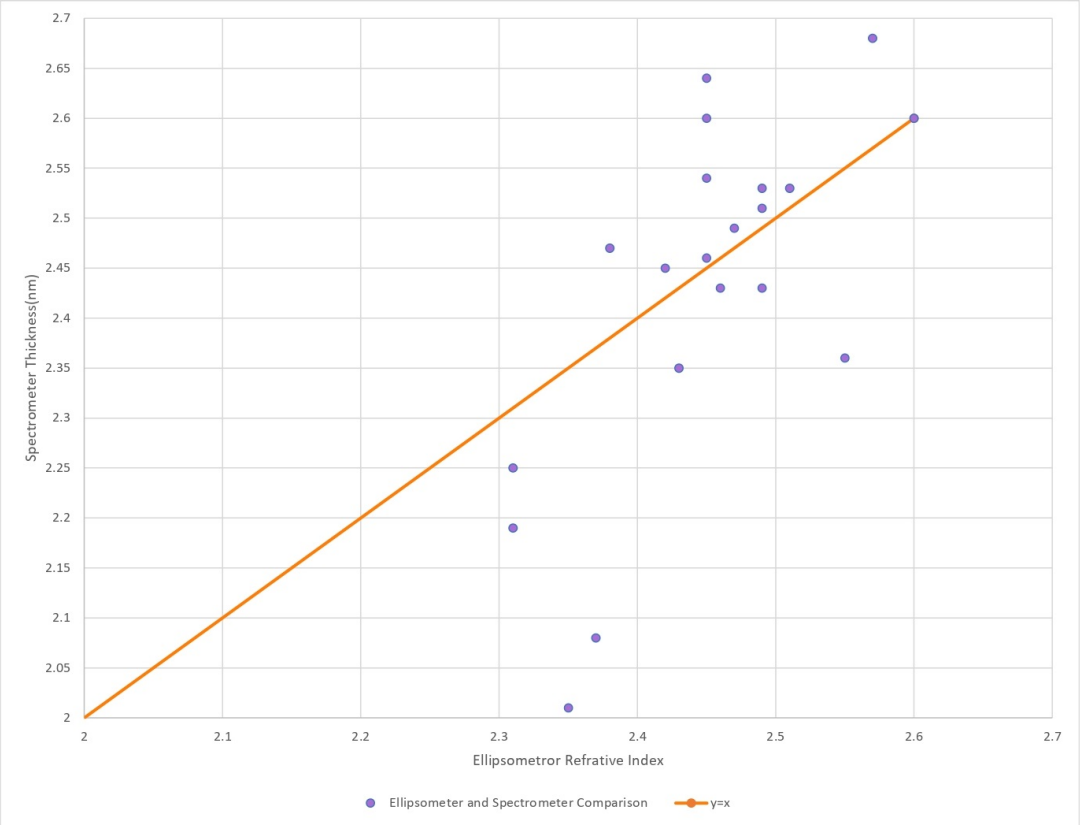

Figure 6.1

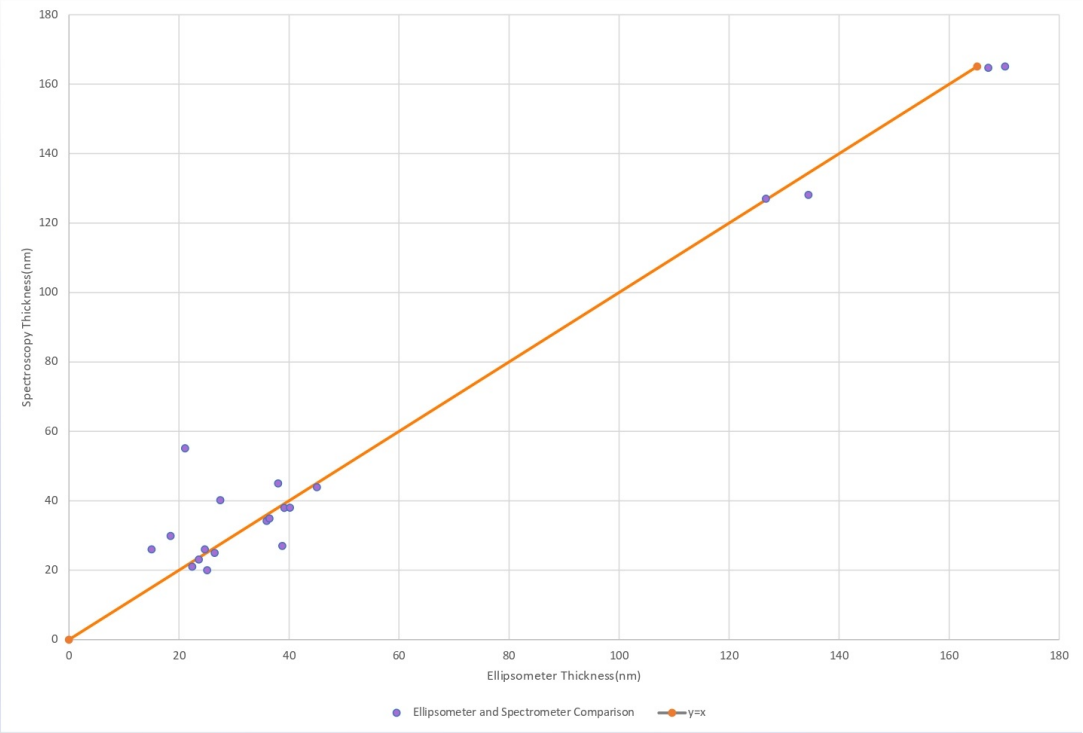
Spectroscopy Thickness(nm)
Ellipsometer Thickness(nm)
0
20
40
60
80
100
120
140
160
180
Ellipsometer and Spectrometer Comparison
y=x

Figure 6.2